

Platinum Single Atoms on Carbon Nanotubes as Efficient Catalyst for Hydroalkoxylation

Hyunje Woo,[†] Eun-Kyung Lee,[‡] Su-Won Yun,[‡] Shin-Ae Park,[‡] Kang Hyun Park,[§]
and Yong-Tae Kim^{‡,*}

[†]Hybrid Materials Solution National Core Research Center (NCRC), Pusan National University, Busan 46241, Republic of Korea

[‡]Department of Energy System, Pusan National University, Busan 46241, Republic of Korea.

*E-mail: yongtae@pusan.ac.kr

[§]Department of Chemistry and Chemistry Institute for Functional Materials, Pusan National University, Busan 46241, Korea

Received June 28, 2017, Accepted August 17, 2017

We report a facile synthesis of Pt single atoms on thiolated carbon nanotubes. To obtain Pt single atoms, it is crucial to treat thiol groups on carbon nanotubes. Pt single atoms on carbon nanotubes were used efficient catalyst for hydroalkoxylation of 3-buten-1-ol or 4-penten-1-ol. Hydroalkoxylation represents an atom-economic route to construct four or five-membered cyclic ethers through intramolecular addition of hydroxyl group. This catalyst exhibited higher catalytic activity than Pt complex and Pt nanoparticles on carbon nanotubes.

Keywords: Platinum, Single atoms, Hydroalkoxylation, Catalyst

Introduction

Oxygen heterocyclic compounds have been much attention as important structural motif in a wide range of biological active molecules such as polyethers, antibiotics, marine macrocycles, and flavor compounds.^{1–4} Among many synthetic strategies, intramolecular addition of an O–H bond (intramolecular hydroalkoxylation) is an atom-economical, and therefore attractive approach for synthesis of saturated oxygen heterocycles.^{5,6} Until now, there have been many efforts to develop efficient catalysts such as brønsted acids, metal salts (Au, Ru, and Pt) and lanthanide complex to remove use of toxic metal ions.^{7–11}

Among them, in particular, the gold(I)-catalyzed intramolecular hydroalkoxylation has drawn extensive interest owing to the potential for both stereospecific and enantioselective transformations.^{12–14} Also, Pt catalysts are introduced for the hydroalkoxylation of direct intramolecular insertion of oxygen, exhibiting better activity and selectivity than Au catalysts,^{15–17} since oxo-philic early- and middle-transition metals as well as Pt metal have strong binding with O-donor ligand and compound containing oxygen. In this paper, we report single Pt atoms on thiolated multiwalled carbon nanotubes (S-MWNTs) to maximize active surface area of catalyst for intramolecular hydroalkoxylation. While transition metal nanoparticles have been much attention for high surface area to volume ratio and surface energy, they show low stability during catalytic reaction due to leaching of metal atoms and morphology change. Our group already reported highly

dispersed single Pt atoms having a highly reduced state on S-MWNTs as supports to overcome these problems.¹⁸ Pt-S-MWNTs catalyst was used as efficient catalyst for intramolecular hydroalkoxylation by increasing activity with O-donor and showed excellent performance and stability compared with Pt nanoparticles and Pt complex.

Experimental

Synthesis of Pt-S-MWNTs Catalysts¹⁸. MWNTs prepared by a conventional CVD method were purchased from Hanwha Nanotech. The MWNTs were purified by refluxing at 70°C for 12 h in 6 M hydrochloric acid (35–37%, Samchun Chemical) after thermally treating raw soot containing MWNTs at 400°C for 2 h in static air. The thiolation of the MWNTs was carried out using an amide bond formation method. Carboxylated MWNTs were obtained by stirring purified MWNTs in a concentrated H₂SO₄/HNO₃ mixture (3:1, 95% and 60% purity, respectively, Samchun Chemical) for 1 h and were chlorinated by refluxing at 70°C for 12 h with SOCl₂ (≥90 v/v%, Samchun Chemical). Then, the remaining SOCl₂ was removed by vacuum evaporation, and the thiolated MWNTs, S-MWNTs, were obtained by stirring at 70°C for 24 h in dry toluene (99.8%, Aldrich, Seoul, Korea) and C₂H₇NSCIH (98.0%, Aldrich). A suspension of S-MWNTs (20 mg) was prepared by ultrasonication in 40 mL of DI water and 3.125 mL of 10 mM H₂PtCl₆·6H₂O (37.5% Pt basis, Aldrich) and 3.125 mL of 10 mM Pd(NH₃)₄Cl₂·H₂O (99.7%, Aldrich) (20 wt %) were added to the suspension. The Pt precursors were

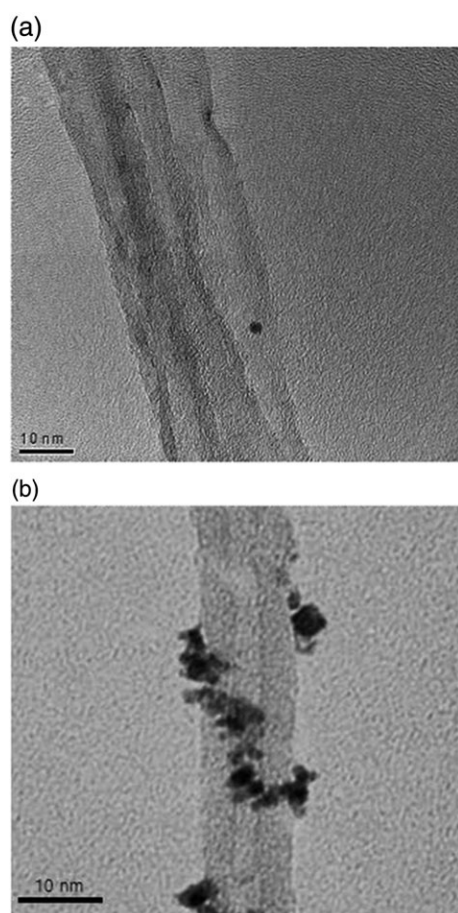


Figure 1. TEM images of Pt SAs on the S-MWNTs (a) and Pt/MWNTs (b).

reduced and formed on the S-MWNTs by stirring them with NaBH_4 (98%, Acros, Seoul, Korea) for 12 h. Then, they were filtered and washed with deionized water and ethanol several times. After evaporation and drying, the 20 wt % Pt precursors supported on S-MWNT, referred to as Pt-S-MWNTs, were obtained. Transmission electron microscopy (TEM; JEM-2011, JEOL, Akishima, Japan), angle-resolved X-ray photoelectron spectrometry (AR-XPS; Theta Probe, cThermo Electron Corporation), and X-ray diffraction (XRD; X'pert PRO MRD; Philips, Amsterdam, Netherlands) were used to analyze the morphology of the catalysts and to confirm the existence of the single atom catalysts. Extended X-ray absorption fine structure (EXAFS) data at the Pt-L3 edge were obtained in transmission mode with the synchrotron radiation of wide X-ray absorption fine structure spectroscopy [10C beam line, Pohang Light Source (PLS)] at room temperature. The spectra were processed using the program IFEFFIT (version 1.2.11, IFEFFIT, Copyright 2008, Matthew Newville, University of Chicago, <http://cars9.uchicago.edu/ifeffit/>) with background subtraction (AUTOBK) and normalization. Fourier transform for EXAFS spectra was performed in the range 2.5–12 Å in k -space and 1–3.5 Å in R -space with the first-shell single scattering paths and k^3 weighting. And the

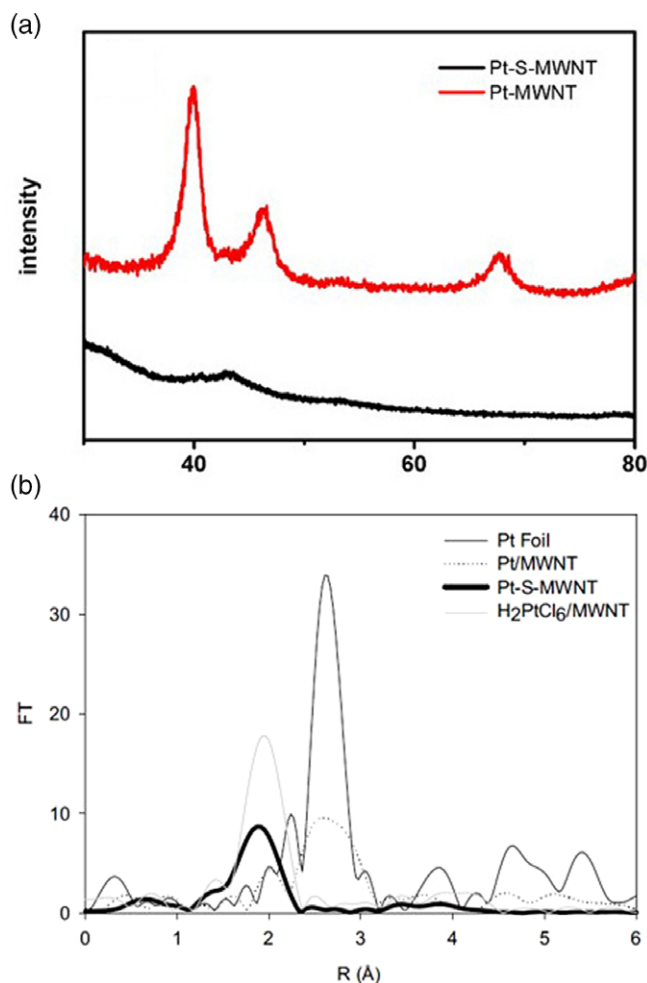


Figure 2. (a) XRD data of Pt-S-MWNTs and Pt/MWNTs. (b) EXAFS patterns showing 1NN Pt-heterogeneous atoms (1.9 Å) of Pt-S-MWNT and 1NN Pt–Pt bond (2.8 Å) of Pt foil.

powder XRD analysis was performed with an Advance X-ray diffractometer (D8 ADVANCE) with $\text{CuK}\alpha$ radiation ($\lambda = 1.54056$ Å). X-ray diffraction data were collected over the 2θ range 10–90° with a step size of 0.02° and a counting time of 0.2 s per step.

Intramolecular Hydroalkoxylation Catalyzed by Pt-S-MWNTs. 4-Penten-1-ol (5 mmol, 99%, Sigma Aldrich, Munich, Germany) and 3-buten-1-ol (6 mmol, 99%, Aldrich) were dissolved in dioxane. Pt-S-MWNTs (2.5 mol % with respect to the substrate concentration) were added with triphenylphosphine (5 mol %, 98.5%, Sigma Aldrich). At this time, the reaction was performed by refluxing at 80°C for 24 h. Product yields from the reaction was measured using gas chromatography (GC, Vernier Mini GC, start temperature 60°C, ramp rate 5°C/min, final temperature 140°C, total length 10.0 min, and pressure 7.0 kPa).

Results and Discussion

Characterization of Pt-S-MWNTs. The synthetic process of Pt-S-MWNTs have previously been reported by our

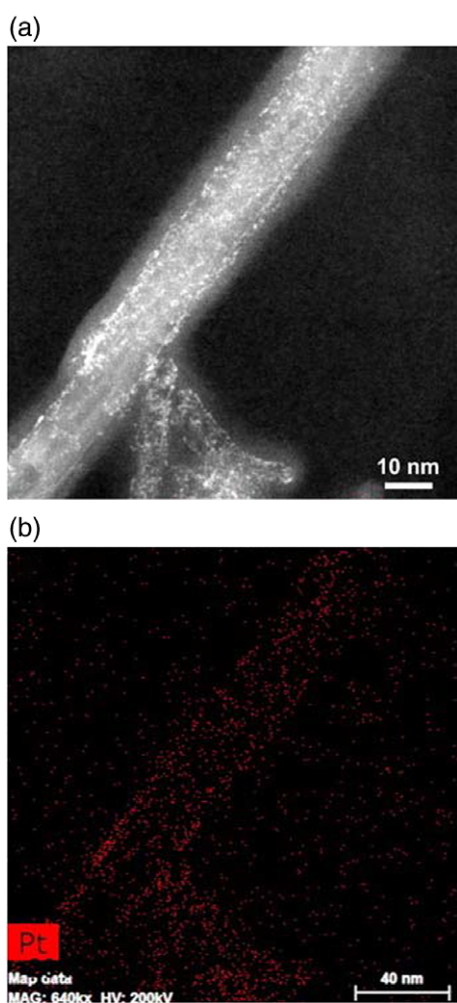
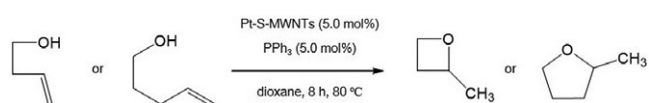


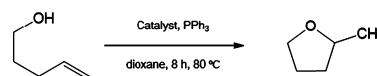
Figure 3. HAADF-STEM image (a) and elemental mapping (b) of Pt-S-MWNT.

group,¹⁸ and therefore we briefly summarize the characterization of the single atom structure. We introduced thiol groups, which have a high affinity for precious metals, on carbon nanotubes to obtain the Pt single atoms on S-MWNTs. The TEM image for Pt-S-MWNTs after the reduction by sodium borohydride of H_2PtCl_6 on the S-MWNT supports is shown in Figure 1(a). Agglomerated Pt nanoparticles are clearly observed on carbon nanotubes which is untreated by thiol groups (Figure 1(b)). In addition, X-ray diffraction measurements did not show any characteristic Pt crystal lattice reflections (Figure 2(a)). These results implies that Pt single atoms are successfully loaded onto the thiolated nanotubes. To confirm the



Scheme 1. Hydroalkoxylation of 3-buten-1-ol or 4-penten-1-ol catalyzed by Pt-S-MWNTs.

Table 1. Effect of catalyst and phosphine on the platinum-catalyzed hydroalkoxylation.



Entry	PPh ₃ (mol%)	Catalyst	Yield (%) ^a
1	0	Pt-S-MWNTs	15
2	2.5	Pt-S-MWNTs	40
3	5	Pt-S-MWNTs	70
4	5	Pt-S-MWNTs	92 ^b
5	0	Pt(COD)Cl ₂	<<5
6	2.5	Pt(COD)Cl ₂	<<5
7	5	Pt(COD)Cl ₂	10
8	0	Pt/MWNTs	<<10
9	2.5	Pt/MWNTs	<<10
10	5	Pt/MWNTs	20

Reaction condition: 4-penten-1-ol (5 mmol), catalyst (2.5 mol %), dioxane (10 mL), 8 h, 80 °C.

^a GC detected yield (%).

^b 7.5 mol % of catalyst was used at 100 °C.

presence of Pt single atoms, EXAFS was conducted (Figure 2(b)). A peak at around 2.8 Å, corresponding to the first nearest neighbor (1NN) Pt–Pt bond, shows the Pt supported on the untreated carbon nanotubes. However, in the case of Pt-S-MWNT, there was no peak at around 2.8 Å, while a clear peak at around 1.9 Å caused by 1NN Pt-heterogeneous atoms. This demonstrates that the supported particles are isolated Pt single atoms surrounded by heterogeneous atoms without any Pt–Pt bond. EXAFS parameters were obtained by fitting the data to a model structure calculated by the FEFF (version 8.3). High-angle annular dark-field scanning TEM (HAADF-STEM) image and elemental mapping were also conducted for confirming Pt single atoms on S-MWNT (Figure 3). However, Pt atoms were aggregated each other when electron beam (200 kV) was irradiated to Pt-S-MWNT sample, resulting in some Pt nanoparticles on S-MWNT (Figure 3).

Hydroalkoxylation (2-Methyloxetane, Tetrahydro-2-methylfuran). To examine catalytic activity of catalysts, hydroalkoxylation of 3-buten-1-ol or 4-penten-1-ol was

Table 2. Effect of catalyst concentration on the Pt-S-MWNTs catalyzed hydroalkoxylation.

Entry	Catalyst (mol%)	Yield (%) ^a
1	1.25	20
2	2.50	40
3	5.00	70
4	7.50	80

Reaction condition: 4-penten-1-ol (5 mmol), PPh₃ (5.0 mol %), dioxane (10 mL), 8 h, 80 °C.

^a GC detected yield (%).

conducted. The higher yield of tetrahydro-2-methylfuran (70%) was obtained than that of 2-methyloxetane (10%) due to less ring strain effect (Scheme 1). Therefore, the catalytic activity of Pt-S-MWNTs, Pt/MWNTs and Pt(COD)Cl₂ was investigated for the hydroalkoxylation of 4-penten-1-ol (Table 1). Preliminary screening to determine the amount of ligand (triphenylphosphine) revealed that 5.0 mol % could efficiently catalyze this reaction (Table 1). The order of the conversion yield is: Pt-S-MWNTs (70%) > Pt/MWNTs (20 %) > Pt(COD)Cl₂ (10%) (Table 1, entries 3,7,10). The Pt-S-MWNTs catalysts are substantially more active than the Pt/MWNTs and Pt(COD)Cl₂, due to the effective activation of olefin in 4-penten-1-ol compared with Pt/MWNTs and Pt(COD)Cl₂.¹⁹ Generally, since platinum-catalyzed hydroalkoxylation involves outer-sphere attack of the hydroxyl group on the platinum-complexed olefin, activation of olefin is crucial to catalyze hydroalkoxylation.¹⁹ The effects of quantity of catalyst (Pt-S-MWNTs) in the reaction were also investigated, with the highest yield obtained for 7.5 mol % (80%) (Table 2). As

expected, 92% of yield was obtained when a reaction temperature was increased to 100°C (Table 1, entry 4). The following conditions proved to be optimal: Pt-S-MWNTs (Pt base: 7.5 mol %), triphenylphosphine (5 mol %) in dioxane at 100°C for 8 h.

The possible origin of the high activity of the Pt-S-MWNT is electron density and ligand effect of the sulfur in the thiol groups. According to previous reports, if the electronic state of the central metal is close to zero, π -bond activation reactions could be easily occurred.^{20,21} The oxidation states of the tested catalysts can be summarized as follows: 0 for Pt/C, almost 0 for the Pt-S-MWNTs, and between +2 and +4 for the ligand complexes (Figure 4(a)). Even though Pt-S-MWNTs are disadvantaged in comparison with Pt/MWNTs regarding their electronic state, much higher surface area of Pt-S-MWNTs for the reaction overcomes this disadvantage. Therefore, for a highly active catalyst for hydroalkoxylation, it is important that the electronic state should be close to zero, and simultaneously the surface area should be as large as possible.

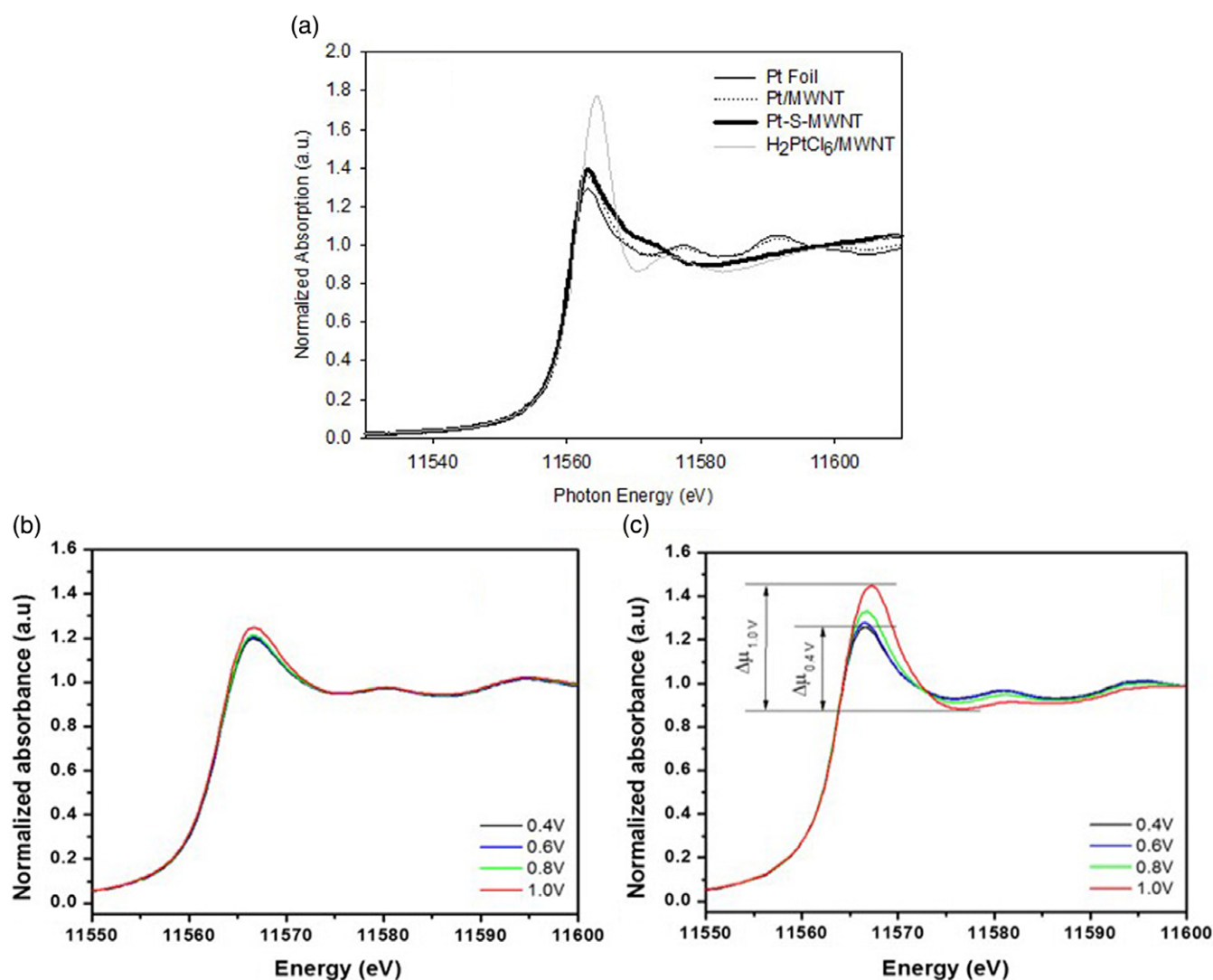


Figure 4. XANES studies to verify the charge compensation process for Pt-S-MWNTs and Pt/MWNTs.

Also, the charge compensation process for Pt-S-MWNTs and Pt/MWNTs was checked to confirm the ligand effect of the sulfur in the thiol groups through X-ray absorption near edge structure (XANES) measurements, in which the oxidized state was simulated by the positive potential application with potentiostat (Figure 4(b) and (c)).²² The Pt-S-MWNTs exhibited a much less degree of white line increase than Pt/C because of a much higher oxidation tolerance of Pt-S-MWNTs. The origin of higher oxidation tolerance of Pt-S-MWNTs was attributed to a charge compensation from sulfur which could rapidly provide the electron, when Pt-S-MWNTs is oxidized.

Conclusion

In conclusion, we demonstrated that the Pt-S-MWNTs have a remarkably high activity for the hydroalkoxylation. Pt-S-MWNTs showed a high activity in comparison with conventional catalysts; 3–7 times higher product yields than Pt/MWNT, Pt complex, respectively. This high activity was attributed to the effective activation of olefin in 4-penten-1-ol compared with Pt/MWNTs. Hence, we firmly believe that Pt-S-MWNTs catalyst can be applied to all catalytic research field for organic reaction.

Acknowledgments. This work was supported by the National Research Foundation (NRF) of Korea grant (2015M1A2A2056556, 2015R1A2A1A10056156, 2013M-1A8A1040703), Nano-Convergence Foundation (R20150-0910), and Korea Institute of Energy Technology Evaluation and Planning (KETEP) grant (2015303003-1510).

References

1. R. Pratap, V. Ram, *Chem. Rev.* **2014**, *114*, 10476.
2. T. D. Sheppard, *J. Chem. Res.* **2011**, *35*, 377.
3. F. Bertolini, M. Pineschi, *Org. Prep. Proced. Int.* **2009**, *41*, 385.
4. R. Badoni, D. K. Semwal, U. Rawat, G. J. Singh, *Nat. Prod. Res.* **2010**, *24*, 1282.
5. S. Fujita, M. Abe, M. Shibuya, Y. Yamamoto, *Org. Lett.* **2015**, *17*, 3822.
6. H. Murayama, K. Nagao, H. Ohmiya, M. Sawamura, *Org. Lett.* **2015**, *17*, 2039.
7. Y. Jeong, D.-Y. Kim, Y. Choi, J.-S. Ryu, *Org. Biomol. Chem.* **2011**, *9*, 374.
8. S. Webster, D. R. Sutherland, A.-L. Lee, *Chem. Eur. J.* **2016**, *22*, 18593.
9. S. Tanaka, T. Seki, M. Kitamura, *Angew. Chem., Int. Ed* **2009**, *48*, 8948.
10. Q. Chen, C. Zhang, C. Wen, J. Fang, Z. Du, D. Wu, *Catal. Commun.* **2014**, *56*, 101.
11. C. J. Weiss, T. J. Marks, *Dalton Trans.* **2010**, *39*, 6576.
12. C. Nagaraju, K. R. Prasad, *Tetrahedron* **2015**, *71*, 9081.
13. W. Zi, F. D. Toste, *Angew. Chem., Int. Ed* **2015**, *54*, 14447.
14. A. Zhdanko, M. E. Maier, *ACS Catal.* **2015**, *5*, 5994.
15. U. Bierbach, M. Sabat, N. Farrell, *Inorg. Chem.* **2000**, *39*, 1882.
16. R. S. Tanke, R. H. Crabtree, *J. Am. Chem. Soc.* **1990**, *112*, 7984.
17. C. J. Besecker, W. G. Klemperer, *J. Am. Chem. Soc.* **1980**, *102*, 7598.
18. Y.-T. Kim, K. Ohshima, K. Higashimine, T. Uruga, M. Takata, H. Suematsu, T. Mitani, *Angew. Chem.* **2006**, *118*, 421.
19. H. Qian, X. Han, R. A. Widenhoefer, *J. Am. Chem. Soc.* **2004**, *126*, 9536.
20. W. Huang, J. H.-C. Liu, P. Alayoglu, Y. Li, C. A. Witham, C.-K. Tsung, F. D. Toste, G. A. Somorjai, *J. Am. Chem. Soc.* **2010**, *132*, 16771.
21. Y. Li, J. H.-C. Liu, C. A. Witham, W. Huang, M. A. Marcus, S. C. Fakra, P. Alayoglu, Z. Zhu, C. M. Thompson, A. Arjun, K. Lee, E. Gross, F. D. Toste, G. A. Somorjai, *J. Am. Chem. Soc.* **2011**, *133*, 13527.
22. S.-A. Park, D.-S. Kim, T.-J. Kim, Y.-T. Kim, *ACS Catal.* **2013**, *3*, 3067.